

**NOTICE WARNING CONCERNING COPYRIGHT RESTRICTIONS:**  
The copyright law of the United States (title 17, U.S. Code) governs the making of photocopies or other reproductions of copyrighted material. Any copying of this document without permission of its author may be prohibited by law.

**The Optimal Design of Pressure Swing Adsorption Systems**

Oliver J. Smith, IV  
and  
Arthur W. Westerberg\*

Department of Chemical Engineering  
and  
Engineering Design Research Center (EDRC)  
Carnegie Mellon University  
Pittsburgh, PA 15213

Prepared for presentation at AIChE Annual Meeting, Chicago, DL  
November 14, 1990  
Paper 68g

To whom correspondence should be addressed.

University Libraries  
Carnegie Mellon University  
Pittsburgh PA 15213\*3890

## Abstract

This work presents a model to determine the annualized cost optimal design of a pressure swing adsorption (PSA) separation system. Design decisions include the number of beds, the operations to use, the scheduling of those operations, and the operating conditions. Operations include adsorption, pressure equalization, blowdown, desorption, and feed repressurization. Operations can be interconnected such as pressurizing one bed by connecting it to another which is to be depressurized.

The capital and operating costs and adsorption behavior of each operation in the operating sequence is approximated by a set of algebraic equations, which, due to the level of error in determining the physical properties, has been found to be sufficiently accurate to characterize the system. The paper presents each of these operation models and the assumptions behind them.

The structure of the model is a mixed-integer nonlinear program (MINLP), the solution of which determines the optimal operating configuration, size, and operating conditions. Designing an "optimal" PSA system to remove methane from a hydrogen stream illustrates the approach.

## Introduction

Pressure swing adsorption (PSA) processes have become a viable alternative for many gaseous separations. Because of their inherent energy efficiency, they can compete with distillation and other heat based separation schemes. To be competitive with these cryogenic methods though, PSA processes must be capable of economically producing products with high recoveries and purities. A system operating using only the most basic PSA steps of pressurization, adsorption, depressurization and desorption is not sufficient to meet these demands (Heck and Johansen, 1978). More inventive designs are used with steps involving bed couplings such as cocurrent and countercurrent repressurizations and depressurizations (pressure equalizations), as well as product repressurization (Yang, 1987).

The expansion of PSA usage depends not only upon the use of highly efficient cycles but also upon the ability to determine an optimal design of the system and its operating conditions. The design and operation of a PSA system is affected by many variables. Improper determination of any of these could lead to increased separation costs due to decreased recovery or increased equipment size (Doshi et al., 1971).

Not much has been published in the literature about the optimization of PSA systems. A

quantitative overview of optimization for a four bed cycle used for hydrogen purification is given (Doshi et al., 1971). For this study, the operating schedule was chosen a priori and the remaining design parameters were improved by the use of experimental data. It clearly illustrated, the numerous trade-offs possible in a PSA system. In another study (Krishnamurthy and Lerner, 1988) the cycle sequence was determined, except for the pressure equalization (PE) steps. The PE steps tested included ones with up to three equalization steps. At most one bed-bed equalization could be followed by up to two bed-tank equalizations. Each different PE sequences was chosen separately and then its optimal operating conditions were determined. One novel bed-bed equalization step that was analyzed used equalizations that were accomplished through both ends of the beds. The concentration profiles in the beds were shown to not move appreciably for this equalization, and a higher recovery proved possible. The results from these studies were used to develop guidelines for selecting pressure equalization steps that could maximize product recovery for other PSA separations.

Both of these studies used an experimental approach to determine the values of the "optimal" design parameters. Thus, although there exists detailed theoretical models for PSA process steps, they were not incorporated into the optimization problem due to their complexity and lack of the necessary property data. A recent study (Banerjee et al., 1990) makes use of exergy analysis to determine the optimal operating parameters of a process, as well as for comparing different configurations. Unlike the above studies, no experimental or laboratory data is used. The optimal configuration or operating point is determined using the minimization of the compressor work per unit mole of product, neglecting the capital costs of the system.

This paper presents work where PSA processes are designed and optimized with respect to the total annualized cost of the process. By the use of this approach, it is hoped that the number and amount of both laboratory and parameter studies necessary to determine the correct operating structure and conditions can be reduced.

## Cyclic Scheduling of Pressure Swing Adsorption Systems

To achieve higher product and pressure recoveries, operations with bed interconnections are used frequently. The use of these operations greatly increases the complexity of the cyclic operating schedule since both beds must begin the connected operation simultaneously and have the same duration. As the complexity increases, it becomes more difficult to formulate even a feasible cyclic schedule, much less an optimal one. This problem has been addressed recently by Chiang (Chiang, 1988) and by Smith and Westerberg (Smith and Westerberg, 1990) for single product systems. In the latter study, we presented a model that structures this problem as an optimization problem.

The basic premise used to formulate the scheduling model is that, if there are  $N$  beds performing the same operations in the same order, then each bed will be operating identically with a time shift  $D$  from another bed's current operation.

$$D = \frac{\tau_{tot}}{N} \quad (1)$$

where  $N$  is an integer and  $x_{tot}$  is the total cycle time, given by the sum of the times of each operation  $x_k$

$M$

If an operation  $O_i$  results from the connection of two beds, then there exists an operation  $O_j$  of the same duration which is the reciprocal operation. The proper scheduling of these dual bed operations requires that the time from the initiation of  $O_i$  to the initiation of  $O_j$  on the same bed be an integer multiple of the interval  $D$ . The following constraints result from this analysis:

$$J_i D = \sum_{k=i}^{j-1} \tau_k \quad (3)$$

which can be written for each such pair of interconnected operations.

The simplest model resulted in a mixed-integer nonlinear program (MINLP). For special cases the nonlinearities may be linearized to reformulate the problem as a mixed-integer linear program (MILP). The algorithm allows time and process constraints to be added or manipulated with ease. The direct solution of the model gives the most desired cyclic schedule.

Since the model was very simple, the objective function used for the above scheduling problem was the minimization of  $N$ , the number of adsorption beds. The scheduling model though, can be modified by adding mass and energy balances as well as correlating costs and operation times to be functions of the design parameters. With these new constraints and an objective function to express total annual costs, a minimum cost design of PSA processes can be accomplished. Of course, the use of the more detailed model necessarily adds many more nonlinear constraints which cannot be linearized. This forces the use of an MINLP model.

The binary existence variables, which were used in the above work to signal the existence or nonexistence of an operation, become very important. They were defined as:

- If  $z_k = 0$  then  $x_k = 0$
- Else; if  $z_k = 1$  then  $x_k \geq \tau_k^{min}$

Thus the first constraint will eliminate an operation if the corresponding binary is zero, whereas the

second constraint will enforce that an operation exists if its binary is one. These binaries also allow interconnected operations to be removed or added to the model due to the following constraints, which enforce Equation 3 if  $z_i \ll 1$  and allow  $J_i = 0$  if  $z_i = 0$ .

$$h_i \leq J_i \leq J_{max,i} \quad \forall i \quad (5)$$

$$\frac{1}{D} \sum_{k=i}^{j-1} \tau_k - J_{max,i} (1 - z_i) \leq J_i \leq \frac{1}{D} \sum_{k=i}^{j-1} \tau_k$$

For the current design model these binaries will be the decision variables used to find the optimal sequence of operations for the system.

## Operation Modeling

The mass and energy balances mentioned above could be added to the algebraic scheduling model in different ways. First, since the original form of the conservation equations are parabolic partial differential equations (PDE's), they could be written as such and then discretized in the spatial and time dimensions to yield an algebraic set of equations. These could then be added to the above model. A second method would be to start with the same PDE's, use equilibrium theory to simplify them to ordinary differential equations (Kayser and Knaebel, 1989), and then discretize to algebraic equations. Both these methods suffer when sharp fronts exist in the adsorber bed due to the large number of discretizations then necessary to insure an accurate solution. Also, these methods assume that the physical constants, such as diffusion coefficients and heats of adsorption, are well enough known so as to prohibit compounding of errors by their use. Much effort and resources would be spent determining the intermediate behavior of the mass and energy fronts while the initial and final profiles are, in most cases, all that are actually needed for design of the system.

Due to these difficulties, we have used simple time integrated balances to describe the initial and final concentration and temperature profiles for each operation of the model. This model allows only average or nominal physical properties to be used, but it still predicts behavior.

The following model is for the purification of a binary (AB) stream, where A is adsorbed and is the impurity and B is considered inert to the adsorbent and is the product. The major assumptions of the model are:

1. Ideal gas behavior.
2. Temperature and mass fronts are both sharp and move with the same velocity.
3. All adsorption and desorption occurs at the adiabatic temperature which is calculated from the corresponding energy balances.

4. All product gas is pure and leaves the bed at the bed's initial temperature.
5. All waste gas (produced during purging) is of the same temperature and composition.
6. The specific heat effects of the metal shell are ignored in the energy balances.

The important equations of the model for each operation are presented below.

### Equations for an Adsorption Operation

Figure 1, shows the essential characteristics of the adsorption model. Adsorption is assumed to

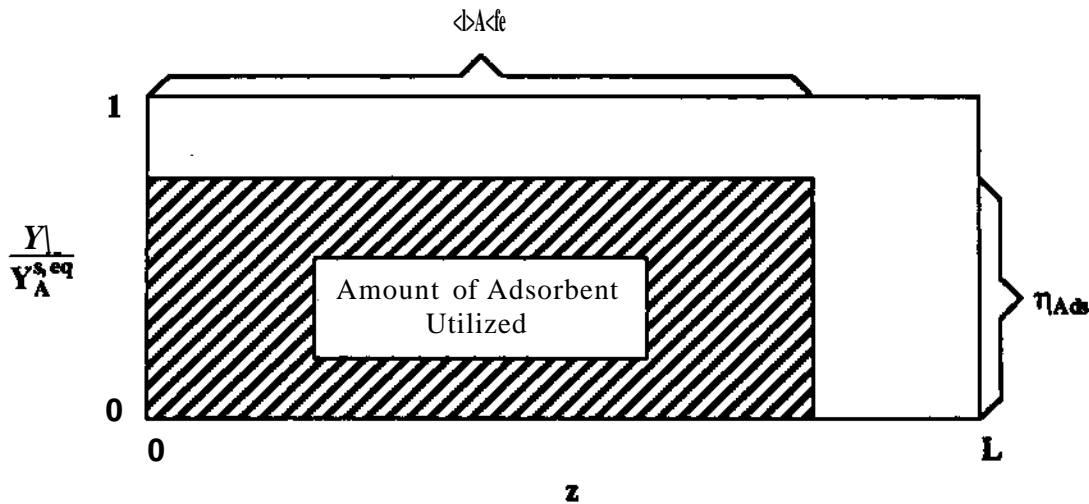


Figure 1: Characteristics of the Adsorption Model

occur at some constant fraction of equilibrium,  $r_i^{\wedge}$ , and use some given percentage of the available adsorbent,  $f_y^{\wedge}$ . Also, the gas in the void spaces of the unused adsorbent,  $(V_b - V^{\wedge}) e$ , is assumed to be pure product. By manipulation of  $T_i^{\wedge}$  and  $\xi_{Ads}$  any type of adsorption behavior can be characterized. For example, if adsorption occurs close to equilibrium with a small mass transfer zone (MTZ) then  $r_i^{\wedge}$  and  $\phi^{\wedge}$  are both approximately 1. If, however, adsorption is not close to equilibrium and the MTZ is large, then,  $\phi^{\wedge}$  and  $T_i^{\wedge}$  would both be less than 1. Use of these parameters is similar to using an efficiency to characterize the performance of a compressor when carrying out preliminary design calculations.

With the use of these parameters, the volume of the bed to be used for adsorption,  $V_{Ads9}$  is calculated by:

$$V_{Ads} = \phi_{Ads} V_b \quad (6)$$

The solid adsorbent in this volume, with an efficiency of  $\eta_{Ads}$ , can adsorb  $m_A^{s,e}$  moles of gas during the course of the operation, which is calculated by:

$$m_A^{s,e} = \frac{\eta_{Ads} q_A V_{Ads} (1 - \varepsilon) \rho_{ads}}{MW_A} \quad (7)$$

The equilibrium isotherm can be given by a variety of theoretical and empirical correlations. In general, any isotherm that is a function of composition, temperature, and pressure, and is of the form  $q_i = f(Y, T, P)$ , can be used. For the example problem given below, a linear isotherm is assumed:

$$q_A = \frac{K_A^{eq} P Y_{A,fg}}{R T^e} \quad (8)$$

At the end of the operation the gas voids in the  $V_{Ads}$  volume are filled with feed gas. The moles of gas in this volume of bed,  $m_{fg}^{v,e}$ , are calculated by:

$$m_{fg}^{v,e} = \frac{P V_{Ads} \varepsilon}{R T^e} \quad (9)$$

The bed is assumed to be equilibrated at a uniform temperature at the start of the operation. The volume of bed where adsorption occurs,  $V_{Ads}$ , rises to a uniform temperature due the heat of adsorption and sensible heat of the incoming stream. Adsorption occurs adiabatically with the temperature of adsorption,  $T^e$ , being determined by the energy balance:

$$m_A^{s,e} H_A + (m_A^{s,e} - m_A^{s,o}) c_{p,A} (T_{fg} - T^e) + (1 - Y_{A,fg}) (m_{fg,Ads}^{in} - m_{fg}^{v,e}) c_{p,B} (T_{fg} - T^i) = V_{Ads} (1 - \varepsilon) c_{p,ads} (T^e - T^i) \quad (10)$$

During the operation, the moles of feed gas processed,  $m_{fg,Ads}^{in}$ , is calculated by:

$$Y_{A,fg} (m_{fg,Ads}^{in} - m_{fg}^{v,e}) = m_A^{s,e} - m_A^{s,o} \quad (11)$$

and the moles of product gas produced during the operation,  $m_{B,Ads}^{out}$ , is calculated by:

$$m_{B,Ads}^{out} = (1 - Y_{A,fg}) (m_{fg,Ads}^{in} - m_{fg}^{v,e}) + \frac{P V_{Ads} \varepsilon}{R T^i} \quad (12)$$

Equations 11 and 12 are used to determine the recovery and economic feasibility of the process.

### Equations for a Pressure Equalization Operation

Since a pressure equalization is a coupled or interconnected operation, the equations must be written for both beds. Here, the bed undergoing a depressurization is signified as 1, and the bed undergoing a repressurization is signified as 2. It is assumed that all of the gas A that enters bed 2 while it is being



repressurized adsorbs onto the solid phase very quickly and is completely adsorbed by the end of step 1, given below.

A pressure equalization operation is modeled by breaking it into three parts:

1. The beds are connected and the gases undergo an adiabatic expansion or compression.
2. The connecting valve is closed.
3. The gas in the beds now equilibrate and establish new temperatures and pressures.

The main equations for step 1 are adiabatic temperature calculations and determination of the moles of gas transferred.

During this step, the pressures are assumed to come to equilibrium, thus:

$$P_1 = P_2 \quad (13)$$

Since the gases have undergone adiabatic expansions or contractions, the final temperature of the feed gas (AB) undergoing the adiabatic expansion in bed 1,  $T_{fg,1}^e$ , can be calculated by:

$$T_{fg,1}^e = T_{fg,1}^o \frac{P_1^e}{P_1^o} \left( \frac{R}{c_{p,fg}} \right) \quad (14)$$

In the same way, the final temperatures of the B and feed gases undergoing an adiabatic compression in bed 2 are, respectively:

$$T_{fg,2}^e = T_{fg,1}^o \frac{P_2^e}{P_1^o} \left( \frac{R}{c_{p,fg}} \right) \quad (15)$$

The moles of feed gas in bed 1 at the end of step 1 is:

$$m_{fg,1}^e = \frac{P_1^e V_b \epsilon}{T_1^e R} \quad (17)$$

and the moles of feed gas into bed 2 is:

$$m_{fg,2}^{in} = \frac{P_2^e V_{fg}^{in} \epsilon}{T_{fg,2}^e R} \quad (18)$$

where  $T_{fg,2}^e$  is given above by Eqn. 16 and  $v\epsilon$  is given by:

$$V_{fg}^{in} = V_b - V_{B,2}^e \quad (19)$$

$$\langle S \rangle \wedge 7 \wedge \quad (CM)$$

The main equations for step 3 are the adiabatic heat balances for beds 1 and 2:

$$V_b (1 - \epsilon) c_{p,ads} (T_1^o - T_1^e) = m_{fg,1}^{v,e} (Y_{A,fg} c_{p,A} + (1 - Y_{A,fg}) c_{p,B}) (T_1^e - T_{fg,1}^e) \quad (21)$$

$$m_{B,2}^{v,o} (Y_{A,fg} c_{p,A} + (1 - Y_{A,fg}) c_{p,B}) (T_{B,2}^e - T_1^e) = V_b (1 - \epsilon) c_{p,ads} (T_2^e - T_2^o) + m_{fg,2}^{in} (Y_{A,fg} c_{p,A} + (1 - Y_{A,fg}) c_{p,B}) (T_2^e - T_{fg,2}^e) \quad (22)$$

and the pressure equilibration (reconciled) equations:

$$r_{ec,1} \quad \frac{1}{\epsilon} \quad (23)$$

$$P_{rec,2} \quad \frac{R}{b \epsilon} \quad (24)$$

### Equations for a Desorption Operation

The desorption operation modeled here combines a blowdown operation and a purge (or desorption) operation. The blowdown operation is essentially the same as that experienced by bed 1 in a pressure equalization operation above, and, since the equations are similar, they will not be given.

Desorption like adsorption is assumed to occur at some constant fraction of equilibrium,  $r|_{Des}$ , and only some percentage of the total amount available to desorb does,  $\xi_{Des}$ . Figure 2, shows the bed concentration profile after the desorption operation. The mole fraction of A in the purge stream, using  $\eta_{Ads}$  and  $\eta_{Des}$ ,<sup>\*</sup> calculated by:

$$Y_A^{out} = \frac{\eta_{Ads} \eta_{Des} q_A T^e}{K_A^{eq} P} \quad (25)$$

The adiabatic desorption temperature is calculated by the following heat balance:

$$V_b (1 - \epsilon) c_{p,ads} (T^o - T^e) = \phi_{Des} m_A^{s,o} H_A + \phi_{Des} m_A^{s,o} c_{p,A} (T^e - T^o) + m_{B,Des}^{in} c_{p,B} (T^e - T_B^{in}) \quad (26)$$

The total amount of product gas (B) that is needed to both purge and fill the void spaces in the bed is:

$$m_{B,Des} = \phi_{Des} \xi_{Des} \frac{m_A}{\epsilon} + m_B \quad (27)$$

and the moles of B needed to fill the gas voids at the end of the operation,  $m^{v,ee}$ , is calculated by:

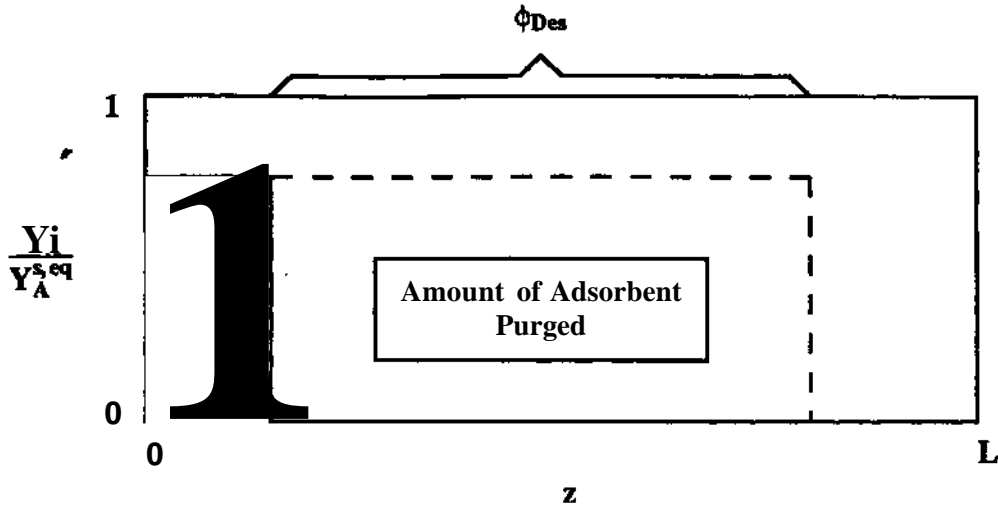


Figure 2: Characteristics of the Desorption Model

$$w_{iB}^{v,e} = \frac{P^* V_b \epsilon}{T^* R} \quad (28)$$

### Equations for Feed Repressurization Operation

The feed repressurization operation is essentially the same as that experienced by bed 2 in a pressure equalization. The equations are similar to those presented above, and they will not be given here except for the equation used to calculate the moles of feed gas needed for the operation,  $m_{FR}^A$ .

$$m_{FR}^A = \frac{V_b \epsilon}{(1 - Y_{A,fg}) R} \left( \frac{P^*}{T^*} - \frac{P^*}{T^*} \right) \quad (29)$$

As in the pressure equalization operation, all the gas A is assumed to adsorb onto the solid phase before the final operation temperature is calculated.

The recovery of the product gas, B, during one cycle can be calculated using Equations 11, 12, 27, and 29 as:

$$Rec_B = \frac{m_{B,Ads}^{out} - m_{B,Des}^{in}}{(1 - Y_{A,fg}) (m_{fg,Ads}^{in} + m_{fg,FR}^{in})} \quad (30)$$

## Process Costs

Since the objective of the optimization problem is to minimize annual cost, it is essential to use accurate correlations for the capital and operating costs. Correlations for the capital costs of the bed metal shell,  $C_{Shell}$ , the compressor,  $C_{Comp}$ , and compressor driver,  $C_{Drive}$  were curve fit from data given by Guthrie (Guthrie, 1974) and Peters & Timmerhaus (Peters and Timmerhaus, 1980). These correlations were then multiplied by the appropriate modular factor and inflation index and summed to yield the total capital cost, in 1987 dollars.

The correlation for the modular cost of the shell was determined to be:

$$C_{Shell} = P^{0.584} (19.73 d l + 14.94 d^2 + 2957) \quad (31)$$

where  $d$  and  $l$  are the diameter and length respectively. The cost of the valves, since for a PSA system it is larger than normal, was included in Equation 31 by tripling the appropriate percentage of base cost in the modular factor. The modular compressor costs were correlated as functions of the inlet flowrate,  $Q_{in}$ , and operating horsepower,  $hp_{Comp}$ , as:

$$C_{Comp} = 14020 Q_{in}^{0.435} \quad (32)$$

$$C_{Drive} = 11.68 hp_{Comp}^{1.61} + 2470 hp_{Comp}^{0.32} \quad (33)$$

The operating costs are given on a per cycle basis and include the costs of purchasing and selling all of the gas into or out of the system during the cycle as well as the cost of compression of the feed gas. The cost/price of the feed and product gases is a specified parameter, and the waste or blowdown gas is sold on the basis of its heat of combustion.

The total annual cost of the system,  $C_{Annual}$ , is then calculated as:

$$C_{Annual} = \frac{C_{cap}}{\tau_{pb}} + (1 - tax) C_{op} + dr tax C_{cap} \quad (34)$$

where  $\tau_{pb}$  is the payback time,  $tax$  is the tax rate on earnings, and  $dr$  is the depreciation rate.

## Model Formulation

The above scheduling, conservation, and cost equations can be combined with additional constraints to form the model to be used for design. Some of these additional constraints are:

1. Constraints on bed diameter and length. The fluidization velocity limit of the bed determines the minimum bed diameter (White and Barkley, 1989). The maximum bed diameter is determined from equilibrium considerations to be the smallest velocity that will still allow a substantial amount of mass transfer.

2. Constraints on the operation time of pressure changes. The operation time,  $z_k^o$ , for an operation undergoing a pressure change was approximated as a linear function of the difference in pressure. Thus, for an operation undergoing a pressure increase we have:

$$\tau_k^o = a_{PC} (P^e - P^o) + \tau_{valve} z_k \quad (35)$$

where  $\tau_{vd/ve}$  is the time required for valve operation at the initialization and termination of the operation. For the below example, a value of  $\tau_{valve} = 1 \text{ s}$  was used.

3. Overall cycle time constraint to ensure closure of the mass balance:

$$\sum_{i \in \text{Ads}} \dot{m}_{fg, Ads} + \sum_{i \in \text{FR}} \dot{m}_{fg, FR} = \dot{m}_{g, tot} \quad (36)$$

where  $\dot{m}_{fg}$  is the molar flowrate of feed gas into the system.

The final model is in the form of an MINLP. The integer variables are the binary existence variables, the cycle integers, and the number of beds. The model description was formulated and debugged using the ASCEND (Piela et al., 1991) modeling system and then set up for optimization using the General Algebraic Modeling System (GAMS) (Brooke et al., 1988).

## Example Problem

It is desired to continuously produce a purified hydrogen stream from a hydrogen/methane waste stream. A PSA system is being considered. Preliminary work suggests considering a PSA system that operates with either zero, one, two, or three pressure equalization operations in the schedule. The overall operation sequence that contains all the possible operations thus is:

- 1:  $O_x$  (Adsorption and production of product gas)
- 2:  $O_2$  (Pressure equalization with low pressure operation  $O_8$ )
- 3:  $O_3$  (Pressure equalization with low pressure operation  $O_7$ )
- 4:  $O_4$  (Pressure equalization with low pressure operation  $O_6$ )
- 5:  $O_5$  (Blowdown and countercurrent purge with product gas)
- 6:  $O_6$  (Pressure equalization with high pressure operation  $O_4$ )
- 7:  $O_7$  (Pressure equalization with high pressure operation  $O_3$ )
- 8:  $O_8$  (Pressure equalization with high pressure operation  $O_2$ )
- 9:  $O_9$  (Repressurize with feed gas)

Operations  $O_5$ ,  $O_9$ , and  $O_x$  must always occur so their binary existence variables are all fixed at 1; whereas, the binary existence variables for operations  $O_2$ ,  $O_3$ ,  $O_4$ ,  $O_6$ ,  $O_7$ , and  $O_8$  are allowed to vary due to the pressure equalization specification above.

Continuous production requires that  $t \gg D$ . The cycle integers for the  $O_2-O_9$ ,  $O_3-O_8$ , and  $O_4-O_7$  interconnected operations will be designated as  $J_1, J_2$ , and  $J_3$  respectively. The parameter values used for the example are given in Table 1, where component A is Methane.

---

$c_{p,A}$	$3.68 \times 10^4 \frac{J}{\text{Kgmole K}}$
$c_{p,B}$	$2.93 \times 10^4 \frac{J}{\text{Kgmole K}}$
$c_{p,ads}$	$8.04 \times 10^5 \frac{J}{\text{m}^3 \text{K}}$
$dr$	$0.125 \text{ yr}$
$ft$	$8.15 \times 10^{13} \frac{\text{Kgmole}}{\text{sec}}$
$H_A$	$8.90 \times 10^8 \frac{J}{\text{Kgmole}}$
$H_B$	$2.86 \times 10^8 \frac{J}{\text{Kgmole}}$
$iff_A$	$12 \times 10^{-2} \frac{\text{JIL}}{\text{Kgmole}}$
$Pr_B$	$3 \frac{\$}{\text{Kgmole}}$
$t_g^n$	$350 \text{ K}$
$T_{fg}$	$298 \text{ K}$
$T_{pb}$	$2 \text{ yrs}$
$tax$	$0.4$
$Y_{A,fg}$	$0.05$
$\epsilon$	$0.44$
$\eta_{Ads}, \eta_{Des}$	$0.95$
$\phi_{Ads}$	$0.95$
$\phi_{Des}$	$1.0$
$\rho_{ads}$	$800 \text{ g}$

---

Table 1: Modeling Parameters used for Example Problem

## Model Solution

To receive further insight into the problem before continuing with the MINLP formulation, the cyclic scheduling problem (Smith and Westerberg, 1990) may be formulated and solved by using reasonable estimates for the process times and other design variables that need to be fixed for this analysis. The binary existence variables were fixed for each specific case, i.e. 0,1,2, or 3 PE steps, and the resulting optimization problem was solved. The model, in this form, is linearizable and thus a mixed-integer linear program (MILP) is all that need be solved. The four pressure equalization cases were solved with the assumption that only the duration of operation one,  $O_v$  is greater than or equal to  $D_9$  (i.e.  $x_x^o = 1$  and for all other operations  $x_k^o \wedge 1$ ). The resulting values for  $N_{min}$  and the cycle integers are given in Table 2. Note that the cycle integer values given in Table 2 are those that result in a feasible schedule given  $N_{min}$  number of beds. There are actually an infinite number of feasible schedules possible for each operating sequence (Chiang, 1988). For example, with one PE operation, two other feasible schedules for  $N$ ,  $J_v$   $J_v$  and  $/_3$  are 4,1,0,0 and 4,2,0,0. The schedule corresponding to  $N_{min}$  though has proved to be optimal for many current PSA systems.

---

<u>#PE's</u>	<u>AT<sub>min</sub></u>	<u>J<sub>1</sub></u>	<u>J<sub>2</sub></u>	<u>J<sub>3</sub></u>
0	2	0	0	0
1	3	1	0	0
2	4	2	1	0
3	5	3	2	1

---

**Table 2:** Integer Variables from Cyclic Scheduling Problem

The results of Table 2 inspire these additional constraints on the cycle integers:

$$J_x \geq J_2 + z_3 \quad (37)$$

$$J_2 \geq J_3 + z_4 \quad (38)$$

These constraints should have been obvious from the problem specification above, since the operations that define the duration of  $J_x$  (i.e.  $O_2$  through  $O_9$ ) totally enclose the operations defining  $J_2$ . Constraints such as Equations 37 and 38 can be written any time all the operations associated with a cycle integer are also all in the set of operations of another cycle integer. Thus, the same analysis as above holds for  $J_2$  and

$J_3$ . The inclusion of these constraints will prohibit the MILP step of the MINLP solution procedure from testing infeasible sets of cycle integers such as  $J_1$  and  $J_2 = 1$ .

Again before solving the overall MINLP problem, we can gain additional insight by using the scheduling results above to further fix the values of the cycle integers and  $N$ , which results in a nonlinear program (NLP) formulation for the model. In fact, if the problem is well enough understood so that the designer is able to prune the infinite number of scheduling possibilities mentioned above, then this solution method of solving a number of MILP's followed by a number of NLP's is all that is necessary. For our example problem, these NLP's were solved, using GAMS and MINOS (Murtagh and Saunders, 1987), to yield initial guesses that were utilized when solving the MINLP formulation. It became apparent at this stage that the formulation is highly nonlinear, having many bilinear terms, and attaining any optima becomes difficult. By manipulating the initial guess and MINOS option parameters, local optima could be obtained.

The overall MINLP problem has the special structure in which the integer variables appear linearly and the continuous variables appear both linearly and nonlinearly. The problem was formulated using GAMS and solved using DICOPT++ (Viswanathan and Grossman, 1990). DICOPT++ is based on the augmented penalty function version of the outer approximation/equality relaxation algorithm (Kocis, 1988). Unfortunately, a solution to this formulation was never obtained using the above software. Using DICOPT++, the relaxed NLP problem and the first MILP master problem were correctly solved to obtain  $x^0, y^0$  and  $x^1, y^1$ , respectively. The difficulties occurred during the solution of the first NLP subproblem. The first NLP subproblem is initialized at the point  $x^1, y^1$  and this point, since it is derived from the linear model, may be "far" from the feasible region. Thus, the linearization of the current NLP constraints may not contain a feasible point. MINOS attempts to relax the bounds on the slacks associated with the nonlinear rows, but only up to 5 times before termination occurs, which is not sufficient for the current problem. This problem could have been overcome by the use of the DICOPT (Kocis, 1988) algorithm which allows the user to specify the initialization point for each NLP subproblem. It was felt by the authors that a simplification of the overall MINLP formulation would be more enlightening.

One simplification is inspired by the differences between the two types of integer variables in the problem: the binary existence variables,  $z_i$ , and the cycle integers,  $N, J_1, J_2, J_3$ . By fixing the values of the binary existence variables, the operating sequence is fixed but the scheduling integers will still cover the infinite number of scheduling possibilities for that structure. The structure of the problem is still an MINLP and since the example considers the possibility of only 0, 1, 2, or 3 pressure equalizations, the



overall MINLP can be expressed by only four of these subMINLP problems. The minimum of these four problems will be the minimum of the overall MINLP problem. This simplification was enough to allow convergence of the subMINLP's with the use of DICOPT++.

The small number of different operating sequences considered in the example allowed it to be expressed by only four subMINLP's. If many operating alternatives were to be considered, the number of subMINLP problems necessary could become large. Under these conditions it becomes necessary to have a more robust MINLP solution procedure. One possibility is to allow the user to interact with the algorithm. By interactively supplying initial guesses and solver parameters, these highly nonlinear problems may be solved.

## Results

The results of the four subMINLP problems are presented in Table 3. The model parameters used were those given in Table 1. As can be seen from Table 3, the largest profit is obtained from the configuration using no pressure equalizations.

<u>#PE's</u>	<u>JL</u>	<u>J<sub>1</sub></u>	<u>J<sub>2</sub></u>	<u>J<sub>3</sub></u>	<u>Cost (1000\$)</u>
0	2	0	0	0	-75.7
1	3	1	0	0	-44.5
2	4	2	1	0	-11.0
3	5	3	2	1	21.6

Table 3: Minimum Costs of the Four Pressure Equalization Configurations

Another fact illustrated by the results in Table 3 is that the scheduling of all four optimal configurations was that given above in Table 2 which resulted from the MILP scheduling problem. In fact, as long as the constraint of  $z^* < 1$  is valid for every operation that it is assumed for, the cycle integers chosen by the scheduling MILP will be the optimal ones. The reason is that the capital costs are a monotonic increasing function of the number of beds whereas the operating costs are invariant to the addition of a bed when in the same scheduling family. The additional bed is not fully taken advantage of since it is not being used to perform another pressure equalization but merely to allow a slightly different schedule to occur.

The results in Table 3 were for a specific set of parameters and hydrogen sale price. It is important to study the effects **that** changes in these parameters has upon the solution. Figure 3 shows the behavior of the optimal **design** due to changes in just the sale price of the product,  $Pr_B$ . Over the range of

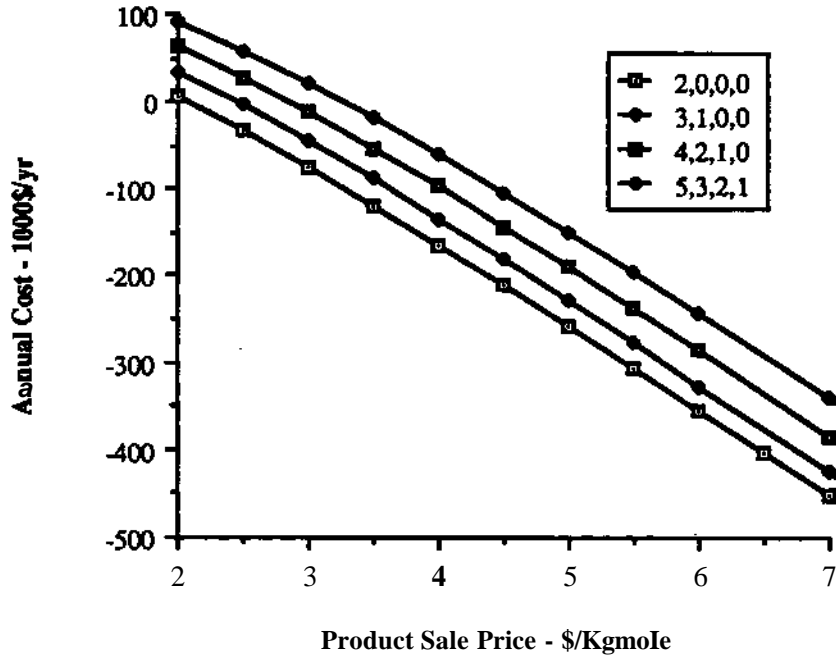


**Figure 3:** Behavior of Optimal Configuration due to Product Price Changes

saleprices considered, (0.25 to 0.9  $\frac{\$}{100SCF}$ ), the configurations are in a strict descending order of cost.

**Due to the increased recovery that a pressure equalization step makes possible**, at  $Pr_B = 12 \frac{\$}{Kgmole}$  the configuration of one pressure equalization step becomes more profitable than no pressure equalization steps. At a larger  $Pr_B$  the two-pressure equalization configuration becomes the most profitable and at an even larger  $Pr_B$  the three-pressure equalization configuration become the most profitable. The large values of  $Pr_B$  necessary for these structural changes are not realistic, but it is important to illustrate that the model predicts the qualitative behavior of the system correctly.

The cost of the capital investment is an important parameter to consider. Figure 4 shows the costs of the four different configurations when capital has become cheaper by 200% (i.e.  $\frac{\%}{p_b} = 6yr$ ). The curves are closer together due to the lower incremental cost of adding another adsorber bed, and the

one-pressure equalization configuration becomes more profitable within the range of saleprices considered.

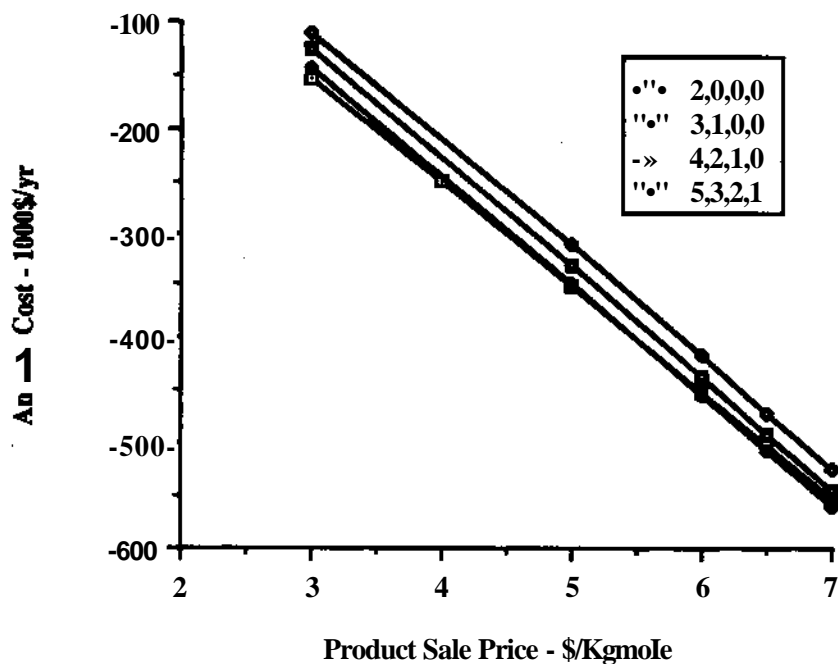


Figure 4: Behavior of Optimal Configuration with  $x_{pb} = 6yr$

Figures 3 and 4 compare the different pressure equalization sequences, but the adsorption and desorption parameters,  $\langle \Delta, r \rangle$ , are held constant for the comparison. This is slightly in error since one would expect to be able to utilize more of the bed for adsorption, i.e.  $\$_{Ads}$  increases, as the number of pressure equalizations increases, since the mass transfer zone, MTZ, becomes sharper. The sharper MTZ allows equilibrium adsorption to occur to a larger bed depth before breakthrough occurs. Thus, the comparisons of Figures 3 and 4 favor the lower number of pressure equalization configurations. Figure 5 illustrates this point further by showing the variation of the cost with 0, 1, 2, and 3 pressure equalizations using a  $\$_{Ads}$  of 0.75, 0.85, 0.90, and 0.95 respectively. Also  $x_{pb} = 4yr$  is used. In the range of saleprices considered the two-pressure equalization configuration becomes more profitable than no-pressure equalizations.

The variation of product recovery due to changes in the adsorption pressure is illustrated in Figure

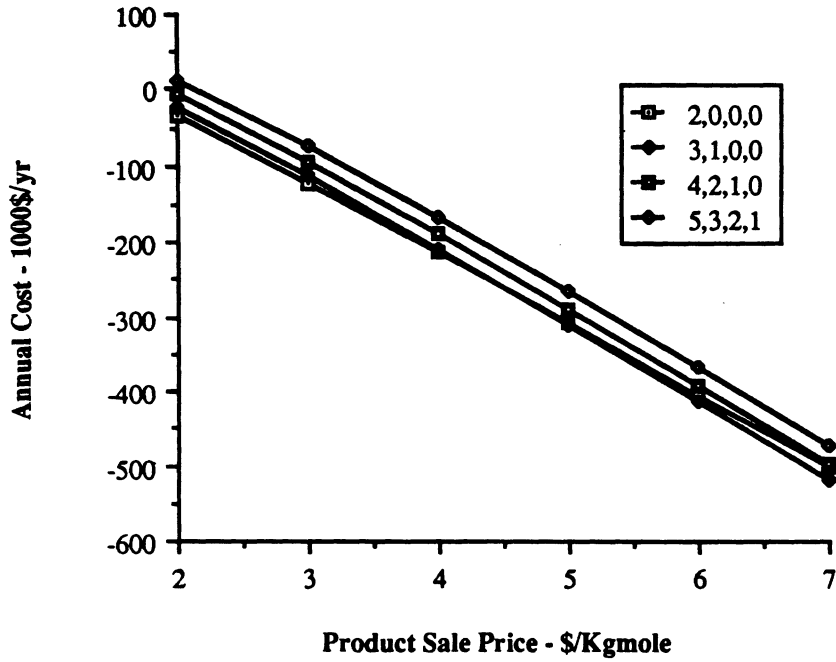


Figure 5: Behavior of Optimal Configuration with different  $\phi_{Ads}$

6. As is expected, the recovery increases asymptotically with pressure. The capital and compression costs increase with pressure also and thus the optimal operating point lies where these competing terms balance. Figure 7 shows the variation of total annual cost due to changes in the adsorption pressure.

## Discussion

The above mass and energy balances for PSA operations have been simplified enough to allow the optimization problem to be of tractable size, yet they still are representative of the actual adsorber behavior. The above MINLP model can then be formulated. The design decisions of the model include the operations, structure, scheduling, and operating conditions of the system.

The parameter studies shown above indicate that both capital and operating costs must be considered during the design process. By basing the design procedure on the minimization of total annual cost, both costs can be properly considered.

The simplified model also allows the competing economic forces to be studied individually. The results of such an analysis can be used to suggest better simplifications for the problem.

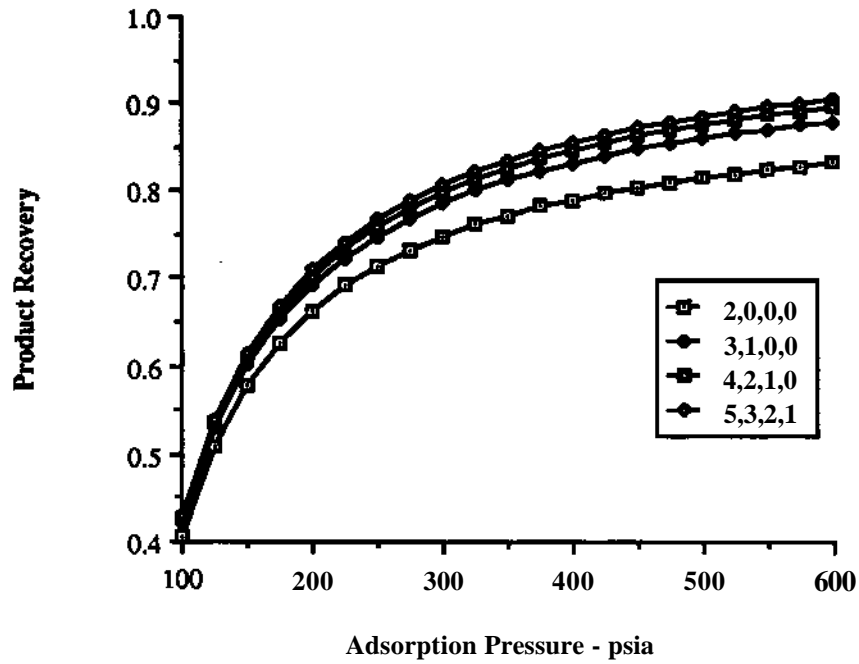


**Figure 6:** Variance in Product Recovery due to Adsorption Pressure Changes

*Acknowledgement* - This research was funded by the Engineering Design Research Center, an NSF funded Engineering Research Center, under grant NSF CDR-8522616.

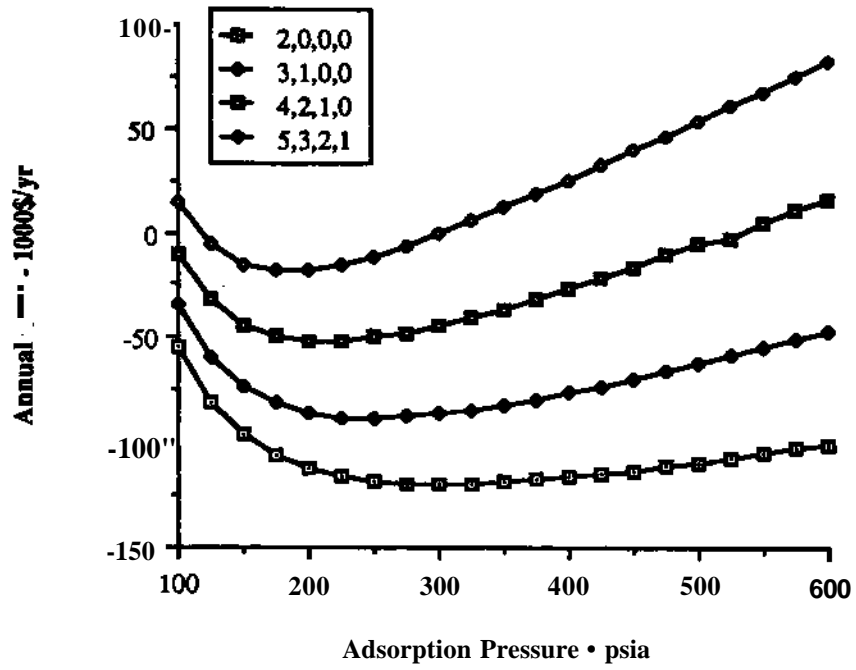


Figure 7: Variance in Total Annual Cost due to Adsorption Pressure Changes

## Notation

$C$	cost - \$
$c_p$	heat capacity - $\frac{J}{Kgmole K}$
$d$	bed diameter - $m$
$D$	cycle shift time ( $= \frac{\tau_{tot}}{N}$ - $sec$ )
$dr$	depreciation rate - dimensionless
$F$	molar flowrate - $\frac{Kgmole}{sec}$
$H$	heat of adsorption - $\frac{J}{Kgmole}$
$hp$	horse power - $hp$
$J_l$	cycle integer $\in \{0, 1, 2, 3, \dots\}$
$K$	adsorption equilibrium constant - $\frac{m^3}{Kgmole}$
$l$	bed length - $m$
$m$	moles - $Kgmole$
$MW$	molecular weight - $\frac{Kg}{Kgmole}$
$N$	number of beds in system $\in \{1, 2, 3, \dots\}$
$O_k$	operation $k$
$P$	pressure - $Pa$
$Pr$	price - $\frac{\$}{Kgmole}$
$Q$	volumetric flow rate - $\frac{ft^3}{min}$
$q_i$	equilibrium amount adsorbed - $\frac{kg_i}{kg_{ads}}$
$R$	gas constant - $\frac{m^3 Pa}{Kgmole K}$
$Rec$	product recovery - dimensionless
$T$	temperature - $K$
$tax$	tax rate - dimensionless

$V$	volume - $m^3$
$Y$	<b>mole</b> fraction - dimensionless
$z_k$	<b>binary existence variable</b>

*Greek letters*

$\epsilon$	<b>void fraction - dimensionless</b>
$\bullet$	bed utilization
$\eta$	efficiency
$\rho$	density - $\frac{k}{m^3}$
$\tau$	time - <i>sec</i>

*Superscripts*

$e$	end (or final)
$eq$	equilibrium
$in$	into operation
$o$	original (or initial) and operation time
$out$	out of operation
$s$	solid (or adsorbent) phase and slack time
$v$	gas (or void) phase

*Subscripts*

$1$	bed <b>1</b> in a <b>dual bed</b> operation
$2$	<b>bed 2</b> in a <b>dual bed</b> operation
$A$	component A
$ads$	adsorbent
$Ads$	Adsorption operation
$b$	bed
$B$	component B (product)
$Des$	Desorption operation



<i>fg</i>	feed gas
<i>FR</i>	Feed Repressurization operation
<i>k</i>	operation <i>k</i>
<i>pb</i>	pay back
<i>rec</i>	reconciled
<i>sh</i>	shell
<i>tot</i>	total

## References

- Banerjee, R., Narayankhedkar, K. G., and Sukhatme, S. P. (1990). Exergy Analysis of Pressure Swing Adsorption Processes for Air Separation. *Chem. Eng. Sci.*, 45(2), 467-475.
- Brooke, A., D. Kendrick and A. Meeraus. (1988). *GAMS: A User's Guide*. Redwood City, CA: The Scientific Press.
- Chiang, A. S. T. (1988). Arithmetic of PS A Process Scheduling. *AIChE J.*, 54(11), 1910-1912.
- Doshi, K. J., Katira, C. H. and Stewart, H. A. (1971). Optimization of a Pressure Swing Cycle. *AIChE Symp. Ser.*, (57(117)), 90-97.
- Guthrie, Kenneth M. (1974). *Process Plant Estimating Evaluation and Control*. Solana Beach, CA: Craftsman Book Co. of America.
- Heck, J. L. and Johansen, T. (1978). Process Improves Large Scale Hydrogen Production. *Hydro. Proc.*, 57(1), 175-177.
- Kayser, John C. and Knaebel, Kent S. (1989). Pressure Swing Adsorption: Development of an Equilibrium Theory for Binary Gas Mixtures with Nonlinear Isotherms. *Chem. Eng. Sci.*, 44(1), 1-8.
- Kocis, G. R. (August 1988). *A Mixed-Integer Nonlinear Programming Approach to Structural Flowsheet Optimization*. Doctoral dissertation, Carnegie Mellon University.
- Krishnamurthy, R. and Lerner, S. L. (1988). Optimum PSA Pressure Equalization Sequence for Argon Separation from Ammonia Purge Gas and Implications for Other Separations. *AIChE Symp. Ser.*, 84(264), 44-53.
- Murtagh, Bruce A and Saunders, Michael A. (1987). *MINOS 5.1 User's Guide*.
- Peters, Max S. and Timmerhaus, Klaus D. (1980). *Plant Design and Economics for Chemical Engineers*. New York, NY: McGraw Hill Book Co.
- Piela, P. C, Epperly, T. G., Westerberg, K. M., and Westerberg, A. W. (1991). ASCEND: An Object-oriented Computer Environment for Modeling and Analysis. Part 1 - The Modeling Language. In press, *Comp. Chem. Eng.*
- Smith, IV, Oliver J. and Westerberg, Arthur W. (1990). Mixed-Integer Programming for Pressure Swing Adsorption Cycle Scheduling. *Chem. Eng. Sci.*, 45(9), 2833-2842.
- Viswanathan J. and Grossmann, Ignacio E. (1990). A Combined Penalty Function and Outer-Approximation Method for MINLP Optimization. *Comp. Chem. Engng.*, 14(1), 769-782.
- White, Donald H. and Barkley, P. Glenn. (1989). The Design of Pressure Swing Adsorption Systems. *Chem. Eng. Prog.*, 85(1), 25-33.
- Yang, R. T. (1987). *Gas Separation by Adsorption Processes*. Boston, MA: Butterworths.